JOURNAL OF GEOPHYSICAL RESEARCH, VOL. 102, NO. D2, PAGES 1727–1737, JANUARY 27, 1997

Detection of cirrus overlapping low-level clouds

Yao Jin[1]
Department of Geosciences, Columbia University, New York

William B. Rossow
NASA Goddard Institute for Space Studies, New York

Abstract. A multispectral method is proposed to detect two-layer cloud systems with an optically thin ($\tau < 1.0$) upper level (Pc < 600 mbar) cloud layer over a lower (600 mbar < Pc ≤ 900 mbar) cloud layer of $\tau > 1.0$, with at least 100-mbar separation. The method uses the results from different high-resolution infrared radiometer sounder (HIRS) channel combinations assuming a single cloud layer in the CO_2-Slicing technique and is valid over both land and ocean. Two months of HIRS data (July 1989 and January 1990) have been analyzed with this method. Globally (excluding regions poleward of 60°) for HIRS field of view (FOV) (about 17 km at nadir) the fraction of such two-layer cloudiness is 25.5% over land and 32.0% over ocean for July 1989 and is 17.8% over land and 25.6% over ocean for January 1990 (this is not the total fraction of two-layer systems). The global distribution patterns of two-layer cloudiness for these 2 months are also presented: the fraction of two-layer cloudiness is larger over ocean than over land; it is larger in the tropics and midlatitude storm zones and smaller in the subtropical zones and marine stratiform cloud regions; over land it is larger in the summer than in the winter at all latitudes; over ocean it is larger in the summer for the northern hemispheric eastern Pacific region while is larger in the winter for all other regions. Qualitative comparisons to surface and upper air observations are also presented and are very encouraging.

1. Introduction

Cloud vertical structure determines the vertical gradients of total diabatic heating/cooling that influence the atmospheric general circulation [*Ramanathan et al.*, 1983; *Webster and Stephens*, 1984; *Slingo and Slingo*, 1988; *Randall et al.*, 1989]. Cloud vertical structure is also indicative of cloud formation processes and of the atmospheric motions that produce clouds [*Cotton and Anthes*, 1989]. Cloud layering also effects water budgets within extratropical cyclones because the storm system's precipitation efficiency is strongly influenced by the vertical distribution of precipitation formation (J. M. Hanesiak et al., manuscript in preparation, 1995).

Currently, satellite cloud retrieval algorithms estimate cloud parameters by assuming a single cloud layer in their radiative transfer model as a practical expedient. Yet in reality, multilayered cloud systems are commonly observed by surface and upper air observations [*Hahn et al.*, 1982, 1984; *Warren et al.*, 1985; *Wang and Rossow*, 1995]. In particular, surface observations show that over ocean cirrus clouds commonly overlie boundary layer convective clouds or stratus clouds and that the probability of finding cirrus with no other clouds is low [*Hahn et al.*, 1982, 1984; *Warren et al.*, 1985; *Tian and Curry*, 1989].

There are very few studies of cloud layering using satellite remote sensing. *Baum et al.* [1994] use multispectral high-resolution infrared radiometer sounder (HIRS) and advanced very high resolution radiometer (AVHRR) data to do multi-level cloud retrievals for a few case studies over ocean at night. In their scheme the spatial coherence algorithm [*Coakley and Bretherton*, 1982; *Coakley*, 1983] is applied to AVHRR 10.8-μm radiances collected within a chosen subregion to detect a lower-level cloud and to determine its mean radiance. Then the HIRS CO_2-Slicing algorithm [*Chahine*, 1974; *Smith and Platt*, 1978; *Menzel et al.*, 1992; *Wylie and Menzel*, 1989] determines the upper level cloud properties using the lower cloud top as the emitting surface. This method works when the low-level optically thick cloud areal extent is much greater than the individual pixel size and requires both completely cloud-covered and completely clear fields of view which restricts the application of the method. Also, the CO_2-Slicing algorithm is only sensitive to cases with an optically thin upper cloud layer (as we show).

Another way of inferring cloud vertical structure by satellite remote sensing is to combine infrared and microwave channels, since high clouds are practically opaque at infrared wavelengths and transparent at microwave wavelengths (*Yeh and Liou*, 1983; *Sheu et al.*, 1996]. *Sheu et al.* [1996] combined special sensor microwave imager (SSM/I) microwave brightness temperature and International Satellite Cloud Climatology Project (ISCCP) visible/infrared (VIS/IR) cloud top properties, along with the European Center for Medium-Range Weather Forecasts (ECMWF) temperature and relative humidity analysis to determine cloud vertical structure and properties over the western tropical Pacific. The scheme utilizes a cloud classification scheme [*Liu et al.*, 1995] that uses both ISCCP cloud top temperature and a microwave index from SSM/I; different cloud classes have different allowed numbers of cloud layers, and the vertical location of the cloud layers is determined based on observational studies and ECMWF relative humidity and temperature profiles. The cloud classifica-

[1]Also at NASA Goddard Institute for Space Studies, New York.

Copyright 1997 by the American Geophysical Union.

Paper number 96JD02996.
0148-0227/97/96JD-02996$09.00

tion scheme [*Liu et al.*, 1995] serves as a guideline for partitioning vertically integrated quantities, such as liquid water path, ice water path, and liquid cloud layer thickness. Since the scheme relies on the ECMWF vertical profile of relative humidity, difficulties were encountered with the relative humidity values above the 700 hPa level, and the spatial resolution of ECMWF analysis was too low to resolve certain type of clouds. Comparing results with the *Hahn et al.* [1982] surface cloud climatology shows generally good results, although several discrepancies are also identified. Comparison of cloud base with lidar cloud base shows good results when tops are below a height corresponding to 700 mbar; however, for classes that include high clouds (e.g., cirrus) along with a lower cloud layer, discrepancies are seen.

In this paper, a multispectral method is proposed to detect those two-layer cloud systems that have an optically thin upper cloud layer over a lower cloud layer. The method is based on the fact that when a lower-level cloud occurs under a semitransparent high-level cloud, the cloud top pressure (Pc) derived using the CO_2-Slicing analysis and assuming a single cloud layer is different for different wavelength combinations. *Baum and Wielicki* [1994] also discuss the retrieved cirrus cloud Pc and effective cloud amount biases produced in multilayer cloud situations using CO_2-Slicing analysis with different HIRS channel combinations and find that the biases are greatest for those using the sounding channels with weighting functions in the lower atmosphere and are least for those using channels with higher-altitude weighting functions. In this paper, we analyze systematically the different sensitivities of the biases in retrieved cloud Pc between different HIRS channel combinations to various cloud and atmospheric properties under multilayer cloud conditions and set criteria for detecting two-layer cloud systems; the upper layer must be optically thin (optical thickness, $\tau < 1.0$), and the top of the lower layer must be low enough (Pc > 600 mbar).

Two months of HIRS data (July 1989 and January 1990) have been analyzed to estimate global distributions of the frequency of thin cirrus occurring over lower-level clouds. Qualitative comparisons to surface and upper air observations are very encouraging. A more definitive test would be comparison to cloud radar results (lidar would not penetrate the lower layer); however, there are not sufficient data available from this relatively new technique to provide a statistically meaningful comparison.

2. Data

HIRS is a 19-channel infrared radiometer (with one visible channel at 0.7-μm wavelength) that is flown on the National Oceanic and Atmospheric Administration (NOAA) polar-orbiting weather satellites. We use the HIRS analysis results from the CO_2-Slicing algorithm of *Wylie et al.* [1994], *Wylie and Menzel* [1989, 1991], and *Menzel et al.* [1992] which uses partially absorbing CO_2 channels from 13 to 15 μm along with one window channel (11 μm) and a water vapor channel. The HIRS field of view (FOV) is about 17 km in size at nadir. To make processing more manageable, the data are sampled at every third pixel on every third scanline, providing results at intervals of about 100 km. The analysis is restricted to observations made at scan angles <25° from nadir to eliminate problems with slant views through the atmosphere. Under cloudy conditions, whenever the signal is larger than the instrument's noise level (valid data), the analysis determines four separate values of cloud Pc from different channel combinations (channels 4/5, 14.2/14.0 μm; channels 5/6, 14.0/13.7 μm; channels 5/7, 14.0/13.3 μm; channels 6/7, 13.7/13.3 μm) and a most representative cloud Pc which best satisfies the radiative transfer equation for all spectral channels (least squares error method) [see *Menzel et al.*, 1983; *Menzel et al.*, 1992]. An effective emissivity (product of the fractional cloud cover and the cloud emissivity) is then derived using the most representative cloud Pc.

In this study, HIRS-retrieved cloud data are mapped to a 2.5° × 2.5° latitude/longitude grid, and monthly statistics are calculated. Two months of data (July 1989 and January 1990) have been analyzed.

3. Sensitivity Tests

3.1. Radiative Model

The radiative transfer model "Streamer" [*Key*, 1996] has been used to simulate HIRS channel radiances under cloudy (single and multilayer) and clear conditions. Streamer is a discrete ordinate model which can compute both fluxes and radiances for any polar and azimuthal angles for 24 shortwave (0.3–4.0 μm) and 105 longwave (4.17–500.0 μm) bands. The only gases considered are water vapor, oxygen, carbon dioxide, and ozone. Each computation is done for a "scene," where the scene can be a mixture of up to eight individual clouds, up to four overlapping cloud pairs, and clear sky. Cloud phase, particle effective radius, and liquid/ice water concentration can be assigned; if cloud optical thickness is input, then cloud physical thickness is computed using effective radius and liquid/ice water concentration specified by the user and the parameterization of *Tsay et al.* [1989]. There are five built-in standard atmospheric profiles: tropical, midlatitude summer, midlatitude winter, subarctic summer, and subarctic winter. For more details about the model, see *Key* [1996].

Streamer's accuracy in clear-sky conditions was tested by computing infrared fluxes for the standard atmospheres of *McClatchey et al.* [1971] and comparing them to calculation by 37 other models presented in the report of the Intercomparison of Radiation Codes in Climate Models (ICRCCM) by *Ellingson et al.* [1991]. In all five standard cases, ranging from tropical to subarctic winter atmospheres, the Streamer-computed fluxes were within 5% and 1 standard deviation of the mean of all the models. *Pinto and Curry* [1996] also compared Streamer's modeled with observed downwelling broadband longwave irradiances for clear sky and find a systematic negative bias of about 3 W/m^2. They also present a clear-sky model intercomparison (six models) that reveals the relatively higher accuracy of Streamer.

In this study, HIRS radiances are simulated using the "band weighting" tables that accompanied the model. For multilayer clouds the upper layer is assumed to be an ice cloud with 25 μm effective spherical particle radius, and the lower layer is a water cloud with 10 μm effective spherical particle radius. (Infrared scattering effects are not very sensitive to the particle shape assumption.) When cloud top pressure and optical thickness are set for each case, the model uses specified liquid/ice water concentrations to compute cloud physical thickness and cloud base location. Most of the sensitivity tests are done for zero satellite zenith angle, but the sensitivity to zenith angles within 30° is small.

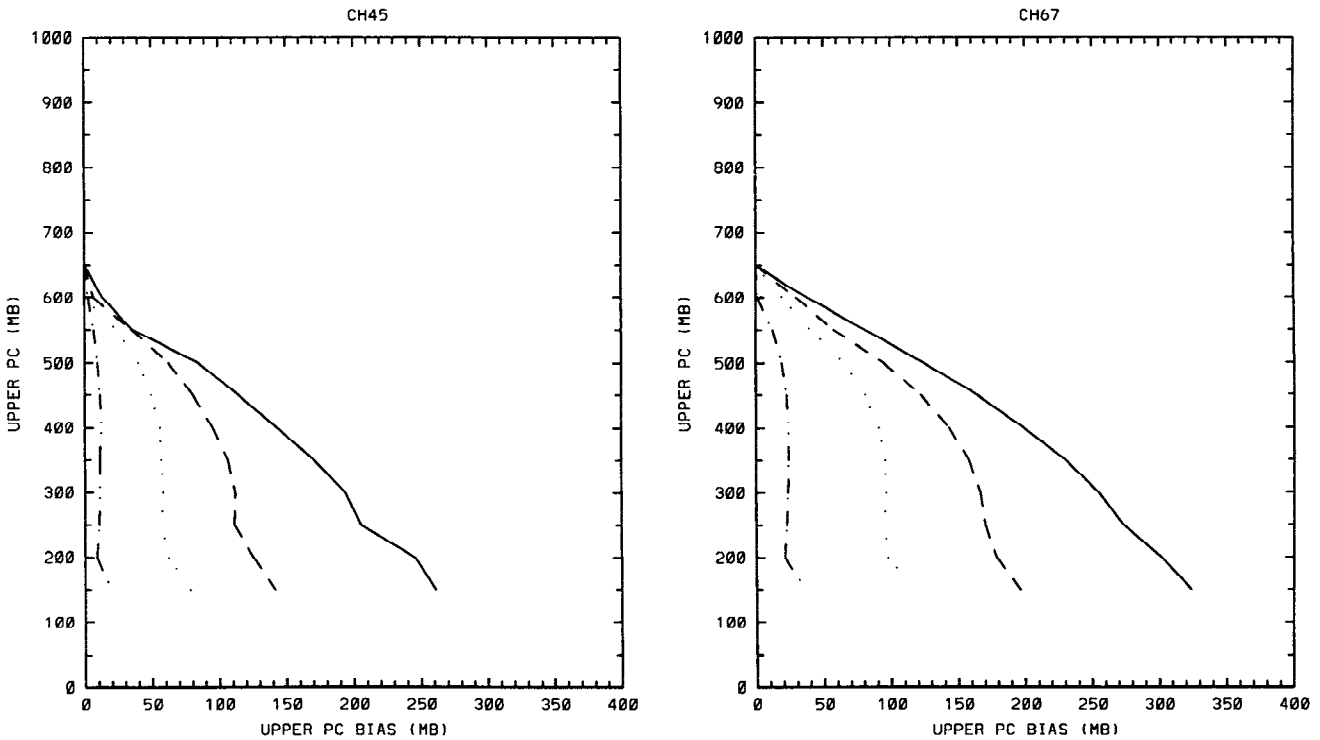

Figure 1. Bias of the retrieved upper layer cloud Pc for two-layer cloud systems with several upper layer cloud τ (solid line, $\tau = 0.2$; dashed line, $\tau = 0.5$; dotted line, $\tau = 1.0$; dash-dotted line, $\tau = 3.0$) as a function of upper level cloud Pc. Results are presented for high-resolution infrared radiometer sounder (HIRS) 4/5 and 6/7 channel combinations for standard midlatitude summer profile. The opaque ($\tau = 10$) lower cloud layer was fixed at 700 mbar.

3.2. Sensitivity Tests

The standard CO_2-Slicing analysis assumes a single cloud layer. We use Streamer to calculate spectral radiances for a variety of two-layer clouds and apply the CO_2-Slicing method to retrieve Pc for the upper cloud. Comparing the retrieved values of Pc with the values specified in the Streamer radiance calculations, we determine the bias in the upper cloud layer Pc produced by the presence of another lower cloud layer. The sensitivity of the upper layer cloud Pc bias and the difference of the bias between different HIRS channel combinations used in the CO_2-Slicing method to variations in the upper and lower cloud layer properties and atmospheric conditions is tested for four standard atmospheric profiles: tropics, midlatitude summer, middle-latitude winter, and subarctic summer. For subarctic winter a near-surface temperature inversion produces ambiguous results.

Figure 1 shows the bias of the retrieved upper layer cloud Pc values for two-layer cloud systems when assuming a single-layer cloud in the CO_2-Slicing method. Results are presented for the HIRS 4/5 and 6/7 channel combinations for several values of upper layer cloud τ and as a function of the true upper layer cloud Pc in the midlatitude summer atmospheric profile. The lower cloud layer is opaque ($\tau = 10$), and its Pc is 700 mbar. Figure 1 shows that the upper layer cloud Pc bias increases with decreasing upper layer cloud Pc and decreasing upper layer cloud τ. Figure 2 shows the same thing as Figure 1, except that the bias is now a function of the lower layer cloud Pc with the upper layer cloud Pc set to 200 mbar. Figure 2 reveals that the upper layer cloud Pc bias increases with decreasing lower-layer cloud Pc to around 600–700 mbar (depending on upper cloud Tau and channel pair), then decreases with the decreasing lower-layer cloud Pc. For other values of the upper layer cloud Pc we get similar results. For other standard atmospheric profiles including tropics, midlatitude winter, and subarctic summer we get similar results with slightly different bias magnitudes.

Both Figures 1 and 2 show that the bias is smaller for sounding channels, the weighting functions of which peak higher in the atmosphere (channels 4/5) because lower-peaking sounding channels have larger surface contributions (other channel combinations give results between those shown). Since the upper layer cloud Pc bias error is not known a priori, we are more interested in the bias differences between different HIRS channel combinations that provide a good indication of the presence of two-layer cloud system with an optically thin higher cloud layer over a lower cloud layer.

Figure 3 shows the retrieved upper layer cloud Pc bias differences between HIRS channel 6/7 and HIRS channels 4/5, 5/6, and 5/7 for several values of upper layer cloud τ as a function of upper layer cloud Pc; the lower-layer cloud is opaque ($\tau = 10$), and its Pc is fixed at 800 mbar. For lower-layer cloud Pc in range 600–900 mbar, we get similar results as in Figure 3. Figure 4 shows the same thing as Figure 3, except as a function of lower-layer cloud Pc with the upper layer cloud Pc fixed at 400 mbar. Both figures are for standard midlatitude summer atmosphere.

Figures 3 and 4 show four features. (1) The bias differences increase with decreasing upper layer cloud τ; they are around 20–40 mbar when upper layer cloud τ is around 1.0 and can be as large as 100 mbar when upper layer cloud τ is around 0.2 for

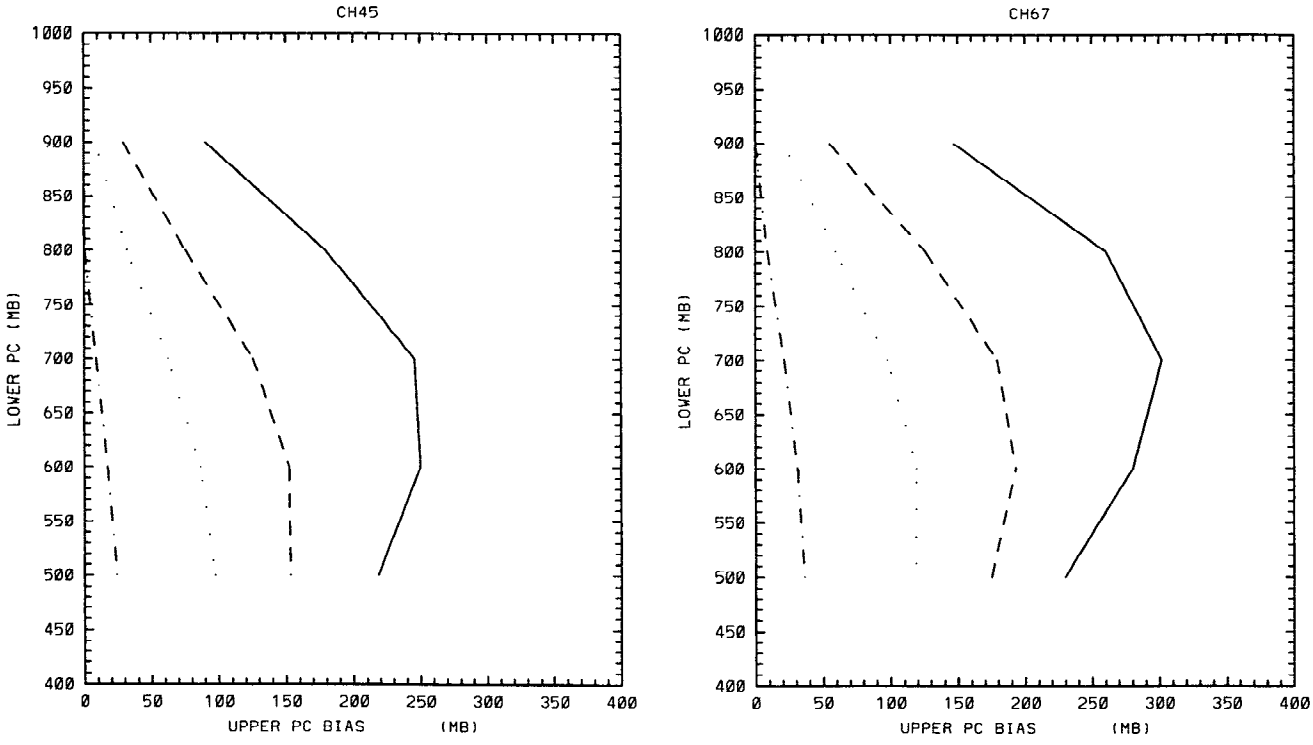

Figure 2. Same as Figure 1, except the bias is a function of lower-layer cloud Pc with the upper cloud Pc fixed at 200 mbar.

the bias differences between channel 6/7 and channel 4/5 and between channel 6/7 and channel 5/6. Consequently, only when the upper layer cloud $\tau \leq 1.0$ can two-layer cloud cases be reliably detected using the bias differences between different channel combinations. (2) The sensitivity of the bias differences to upper layer cloud Pc is small as long as upper layer cloud Pc $\leq$ 500–600 mbar. (3) The bias differences become detectable when lower-level cloud Pc is around 600 mbar and increase as the lower-level cloud Pc increases to around 800–900 mbar (depending on upper layer cloud τ). The bias differences decrease to zero as the lower-level cloud Pc increases to the surface pressure (Pc = 1000 mbar) as it should because such a low cloud is indistinguishable from the surface as in a single-layer cloud situation. As a result, in order for the two-layer cloud cases to be detected, the lower cloud layer must be located between 600 and 900–950 mbar. (4) The bias differences between channel 6/7 and channels 4/5, 5/6, and 5/7 decrease progressively. This progressive decrease among all four channel pairs is important in detecting two-layer cloudiness to avoid detection errors caused by random errors in the results. The channel pairs 6/7 and 4/5 are the best combinations for detecting two-layer cloudiness since the bias differences between these pairs are largest. The differences between channel 6/7 and channel 5/6 are similar to those between channel 6/7 and channel 4/5, so when channel 4/5 data are not available, we can use channel 5/6 data instead. We did the same tests for other standard atmospheric profiles, and the above results are similar for all four standard atmospheric profiles, with slightly different magnitudes in the bias differences.

Figures 3 and 4 show cases with the lower-layer cloud τ fixed at 10.0. To test the sensitivity of the bias differences to the lower-layer cloud τ, we did the same calculations as above with the lower cloud τ set to 3, 1, and 0.5. These results show that the bias differences hardly change when lower-layer cloud $\tau >$ 1.0. The global distribution of lower cloud τ values obtained in the ISCCP (4–7 km FOV) data set [*Rossow and Schiffer*, 1991] has a majority of low clouds with $\tau > 1.0$. The statistics of ISCCP low-level clouds for the months July 1989 and January 1990 show that only 16–17% of low-level clouds have $\tau < 1.4$. For the HIRS FOV (about 17 km at nadir) this frequency would be higher due to its larger FOV. Consequently, most two-layered cloud cases will have a thicker lower cloud layer.

For all calculations above we used the ocean surface emissivity. For HIRS channels 4, 5, 6, and 7 wavelengths the emissivity of terrestrial materials varies within the range 0.9 ~ 1.0 [*Buettner and Kern*, 1965; *Salisbury and D'Aria*, 1992]. To test the sensitivity of bias differences to surface emissivity, we repeated the calculations in Figures 3 and 4 with surface emissivity fixed at 1.0 and 0.9 for the four standard atmospheric profiles. Changes of surface emissivity from 0.9 to 1.0 cause negligible (<20 mbar) changes of bias differences, so the conclusions from sensitivity tests above are applicable over land also.

When single-layer partial cloud cover occurs within HIRS FOV, the cloud Pc estimated by CO_2-Slicing algorithm would have similar bias derived from different HIRS channel combinations and thus would not cause false detections as two-layer cloud system. For above tests (and in the analysis) we assume overcast cloud conditions for both cloud layers. For broken clouds we repeated the calculations in Figure 3 with different overlapping cloud fractions and find that for overlapping cloud fractions larger than 0.5 the bias error difference between channel 4/5 and channel 6/7 is larger than 40 mbar for an upper layer cloud $\tau < 0.5$; for an upper layer cloud $\tau = 1.0$ the bias difference decreases from 40 mbar for total overlap to 20 mbar for 0.5 overlapping fraction.

From the sensitivity tests of the upper cloud Pc bias differ-

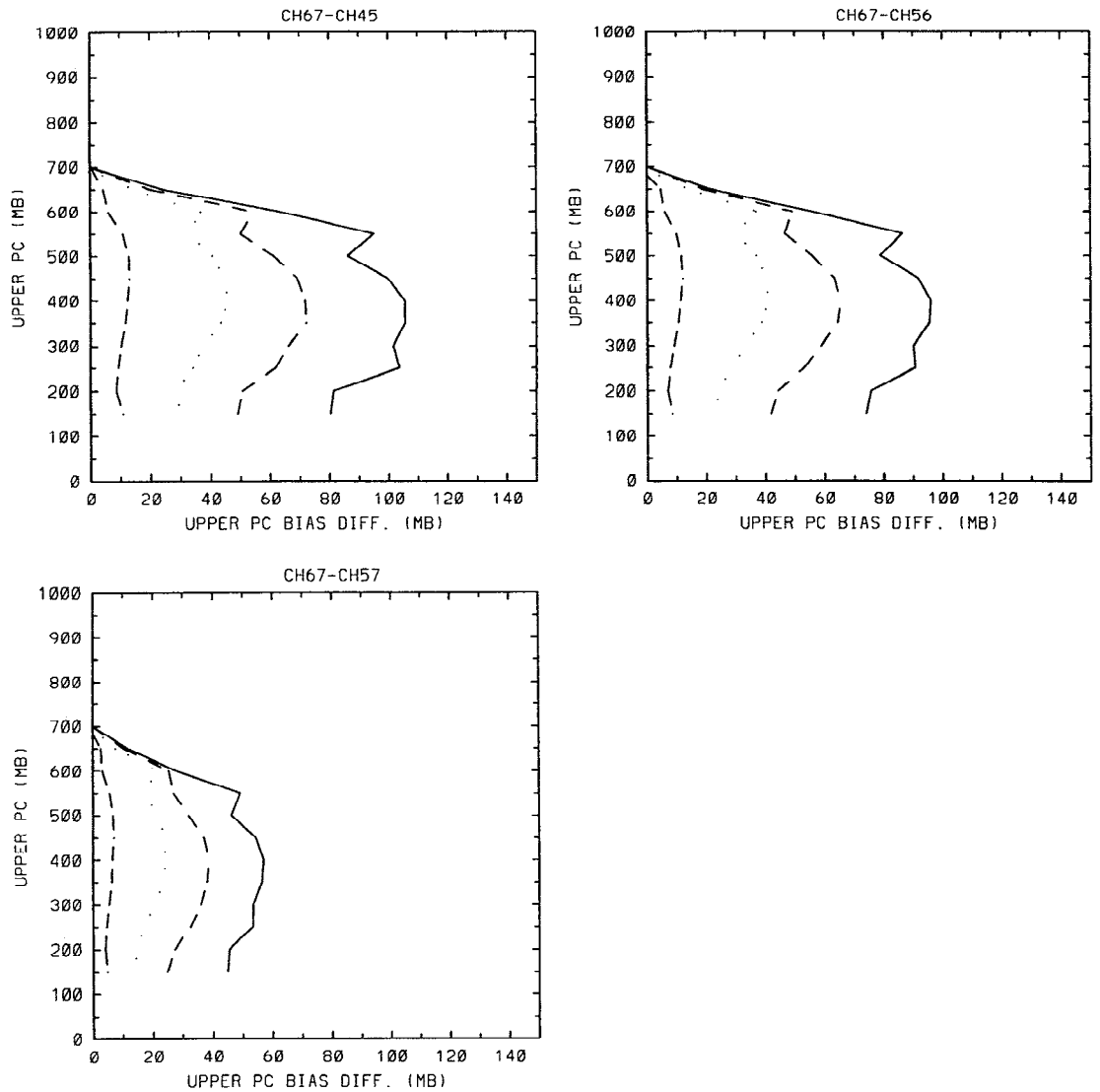

Figure 3. Bias differences for two-layer cloud system between retrieved upper layer cloud Pc values using HIRS channel 6/7 and HIRS channel 4/5 (top left panel), 5/6 (top right panel), 5/7 (bottom panel) for several upper cloud τ (solid line, $\tau = 0.2$; dashed line, $\tau = 0.5$; dotted line, $\tau = 1.0$; dash-dotted line, $\tau = 3.0$) as a function of upper layer cloud Pc. The lower-layer cloud is opaque ($\tau = 10$) and is fixed at 800 mbar. Results are presented for atmospheric standard midlatitude summer profile.

ences to variations of cloud and atmospheric parameters we can define the range of parameters for which two-layer cloud systems are detectable using the upper layer cloud Pc differences retrieved from different HIRS channel combinations. This range is also linked by the random error sources [*Menzel et al.*, 1992] to bias error differences between channel 4/5 and channel 6/7 larger than about 40 mbar. Figure 5 shows a schematic of this range as a function of cloud Pc and cloud τ. The shading represents the allowed range of the upper level cloud, and the hatching represents the allowed range of the lower-level cloud. The higher cloud layer must be located higher than the 600 mbar level with $\tau < 1.0$, while the lower cloud layer must be located between 600 and 900 ~ 950 mbar with $\tau > 1.0$. There also must be a separation of about 100 mbar between the two cloud layers. *Wang and Rossow* [1995] studied the cloud vertical structure from upper air observations at 30 sites over ocean and found that 56% of clouds are multilayered with half of the multilayered clouds composed of two layers. For the two-layer cloud systems the lower layer occurs mostly below 3 km (Pc $\approx$ 700 mbar) with a peak frequency at 1 km (Pc $\approx$ 900 mbar), and the higher layer occurs over a wide range from 2 km (Pc $\approx$ 800 mbar) to 11 km (Pc $\approx$ 230 mbar) with a peak frequency at around 6 km (Pc $\approx$ 470 mbar). The separation distance between two consecutive layers in multilayered cloud systems has a mean value of 2.1 km, and more than two thirds of the clouds have separation distance larger than 1.0 km. Wang and Rossow's results suggest that our method can detect a large fraction of the multilayer cloud systems as long as the optical thickness of the upper layer clouds is not too large. Surveys of the optical thickness distributions of high-level clouds based on ISCCP, HIRS, and stratospheric aerosol and gas experiment II (SAGE II) all suggest that more than 30–40% of all upper level clouds have $\tau \leq 1.4$ [*Liao et al.*, 1995a, b; *Jin et al.*, 1996]. Wang and Rossow also note that their results probably underestimate the frequency of cases with optically thin upper layer clouds.

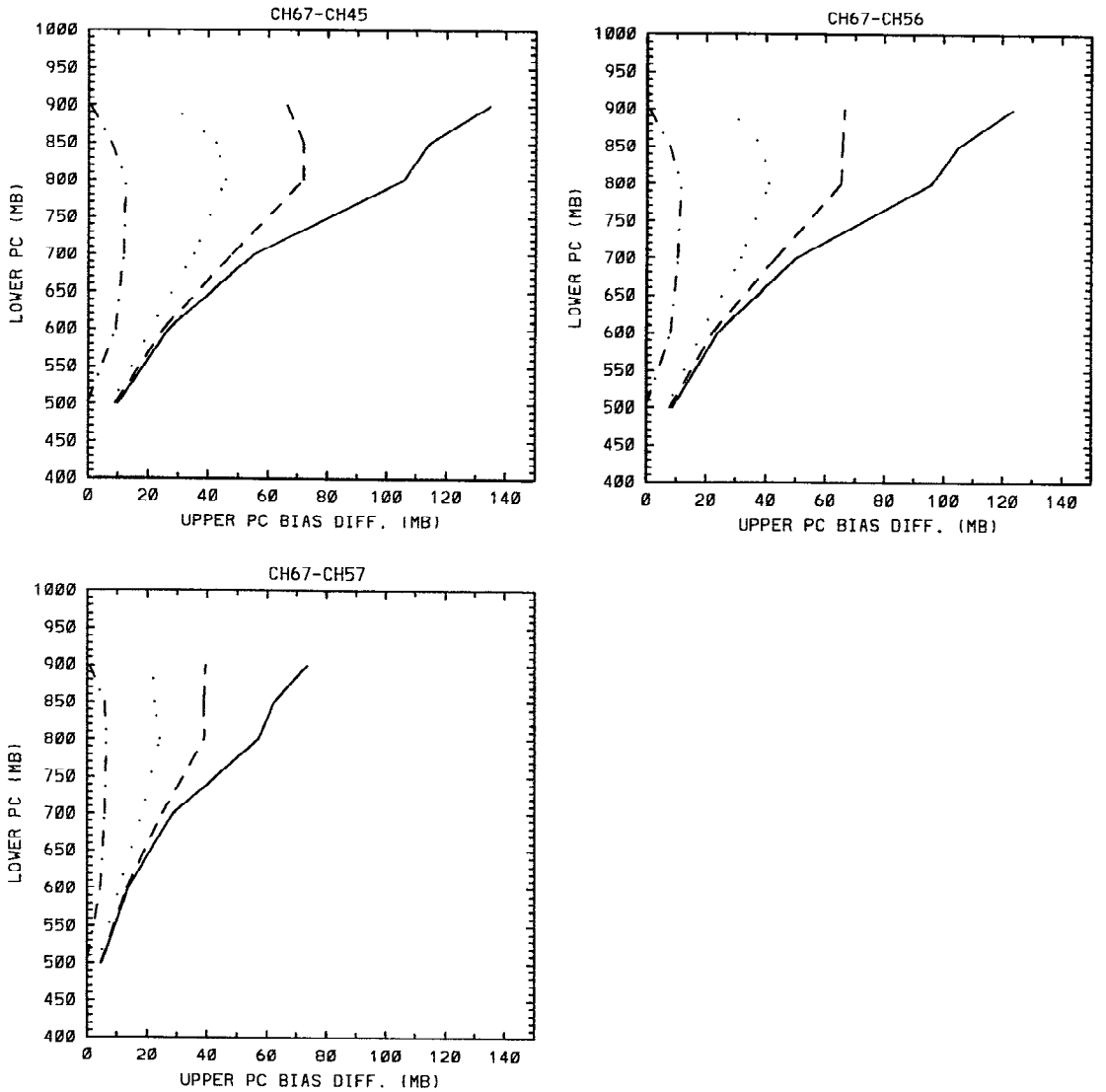

Figure 4. Same as Figure 3, except the bias differences are now a function of lower-layer cloud Pc with the upper layer cloud Pc fixed at 400 mbar.

4. Data Analysis

4.1. Data Analysis Method

On the basis of the sensitivity study we propose a method for detecting those two-layer cloud systems that are composed of an optically thin upper cloud layer over a lower cloud layer. For each cloudy pixel reported in the HIRS data we examine the cloud Pc values from the four different channel combinations (channels 4/5, P45; channels 5/6, P56; channels 5/7, P57; channels 6/7, P67): when all Pc values are valid (or all but P45), P45 ≤ P56 ≤ P57 ≤ P67 (or P56 ≤ P57 ≤ P67), and (P67–P45) > threshold (or (P67–P56) > threshold), then we classify this pixel as a two-layer cloudy scene. The threshold is 0 mbar in this study, but it could be between 0 and 50 mbar because the results show only very small differences for thresholds in this range (less than 2% for all latitude zones). This insensitivity to the threshold between 0 and 50 mbar is related to the Pc retrieval interval (~50 mbar) employed in the HIRS analysis. For each map grid box for each month we count the frequency of occurrence of two-layer cases and divide it by the frequency of total cloudiness, which results in the fraction of two-layer cloudiness (this is not the total two-layer cloud frequency because we cannot distinguish one and two-layer systems with a thick upper layer).

4.2. Data Analysis Results

Globally (excluding regions poleward of 60°) for HIRS FOV (about 17 km at nadir) the frequency of the two-layer cloudiness is 16.9% over land and 25.5% over ocean for July 1989 and 12.4% over land and 20.4% over ocean for January 1990. The two-layer fraction is 25.5% over land and 32.0% over ocean for July 1989 and 17.8% over land and 25.6% over ocean for January 1990. This is close to the fraction of two-layer clouds (~28%) over ocean estimated by *Wang and Rossow* [1995]. Their results probably underestimate the fraction by missing the cases when the upper cloud layer is optically thin, but our results miss the cases with optically thick upper cloud layers.

Figure 6 shows the global distribution of the fraction of the two-layer cloud systems for January 1990 (Figure 6a) and July 1989 (Figure 6b) from our analysis as deviations from the global mean values. Figure 7 shows the result derived from

surface observations [*Hahn et al.*, 1982] for winter (December, January, and February) (Figure 7a) and summer (June, July, and August) (Figure 7b). The global mean value is 24.3% for January 1990 and 31.0% for July 1989 for the HIRS analysis; for surface observations it is 45.9% for winter and 50.4% for summer. The fact that our global mean value is about half that of the surface observations is consistent with the fact that about half of all high level clouds (Pc < 440 mbar) have $\tau > 1.4$ (from our HIRS analysis). The geographical distribution and seasonal variation pattern are very similar. The spatial correlation (both mapped to 10° × 10° grid) between HIRS and surface observation patterns of two-layer cloud fractions is 0.53 for summer and 0.65 for winter. Consequently, over the Southern Oceans where there are no surface observations our results provide the first estimates of the geographical and seasonal variation patterns.

Figure 8 shows the latitudinal distribution of the two-layer fraction over land and over ocean for July 1989 (Figure 8a) and January 1990 (Figure 8b). The fraction of two-layer cloudiness is larger over ocean than over land, which agrees with the surface observations that there is much more low-level cloudiness over ocean than over land and thus cirrus are much more likely to be found alone over land than over ocean [*Hahn et al.*, 1982; *Warren et al.*, 1985]. Figure 8 also shows that the fraction is larger in the tropics and midlatitude storm zones and smaller in the subtropical zones and marine stratiform cloud regions (cf. Figure 6). Over land the fraction is larger in the summer than in the winter at all latitudes, probably because greater convective activity in summer generates more low clouds [*Warren et al.*, 1985]. Over ocean the seasonal changes are more complicated: the fraction is larger in the summer in the tropics, but for the subtropics and midlatitude zones it is larger in the summer for the northern hemispheric eastern Pacific regions, while it is larger in the winter for all other regions. Surface observations show that over ocean cirrus commonly overlie boundary layer convective clouds or stratus clouds [*Hahn et al.*, 1982; *Warren et al.*, 1985; *Tian and Curry*, 1989]. *Hahn et al.* [1982, 1984] show that cirrus (Ci) occurs more frequently with cumulus (Cu) or cumulonimbus (Cb) clouds at low latitudes (30°S–30°N) and with stratus clouds at high latitudes over ocean. Therefore a larger fraction of multilayered clouds is likely to be associated with the maximum frequency of occurrence of Cb and Cu in summer at low latitudes and a higher probability of Ci also being present in summer than in winter given a low convective cloud type (Cu or Cb) [*Wang and Rossow*, 1995]. The seasonal variation patterns over the subtropical and midlatitude oceans are probably produced by two compensating factors [*Wang and Rossow*, 1995]: larger frequency of stratus clouds in summer [*Klein and Hartmann*, 1993] and more multilayered cloud systems associated with frontal activity in winter. These trends also agree with *Wang and Rossow* [1995] upper air observations which show that a tropical station has more multilayered clouds than at other stations, the least frequent multilayered clouds occur at the two subtropical eastern Pacific stations, the frequency of multilayered clouds is larger in summer than in winter at low latitudes, negligible seasonal variations appear at the North Atlantic stations, and more multilayered clouds appear in winter at the two subtropical eastern Pacific stations.

Over the Southern Oceans where surface and upper air observations are not available, Figures 6 and 8 reveal that the fraction of two-layer cloudiness in the winter is about 10% larger than in the summer. Obviously, this is not caused by a seasonal change of the contrast between sea surface and land temperatures, so it must be related to a seasonal change of atmospheric general circulation.

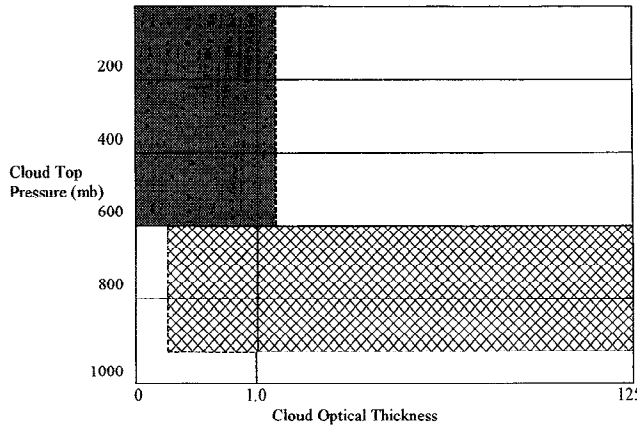

Figure 5. Diagram of the range of two-layer cloud system properties which can be detected by the multispectral method developed in this paper, as a function of cloud τ and Pc. The shaded area represents the range of upper level cloud, and the hatched area represents the range of lower level cloud.

To study the fraction of high-level clouds which have low-level clouds below, we divide the frequency of two-layer cloudiness by the frequency of HIRS high-level clouds (Pc ≤ 440 mbar). Globally (excluding regions poleward of 60°) this fraction is 53.0% over land and 76.4% over ocean for July 1989 and is 37.65% over land and is 58.7% over ocean for January 1990. This fraction value also varies geographically and seasonally; generally, it is larger over tropics and midlatitude storm zones than subtropical zones and is larger over ocean than over land. It has its largest value (almost 100%) over Southern Ocean winter (July 1989). When a low-level cloud layer occurs below optically thin high-level cloud layer, the high-level cloud properties, retrieved assuming a single-layer cloud, are biased [*Baum and Wielicki*, 1994]. Considering the large fraction of high-level clouds with low-level clouds below, it is important to calibrate the high cloud properties for two-layer cloud cases in major cloud climatologies like ISCCP [*Liao et al.*, 1995a, b; *Jin et al.*, 1996].

5. Summary and Discussion

A multispectral method is proposed to detect those two-layer cloud systems that have an optically thin ($\tau < 1.0$) upper level (Pc < 600 mbar) cloud layer over a lower (600 mbar < Pc < 900–950 mbar) cloud layer with at least 100-mbar separation. The method is developed by studying the sensitivity of the difference of upper layer cloud Pc retrieved from different HIRS channel combinations assuming a single cloud layer in the CO_2-Slicing technique. The method is valid over both land and ocean.

Two months of HIRS data (July 1989 and January 1990) have been analyzed according to this method. Globally (excluding regions poleward of 60°) for HIRS FOV (about 17 km at nadir) the fraction of two-layer cloudiness is 25.5% over land and 32.0% over ocean for July 1989 and 17.8% over land and 25.6% over ocean for January 1990. The fraction is larger over ocean than over land; it is larger in the tropics and midlatitude storm zones and smaller in the subtropical regions and

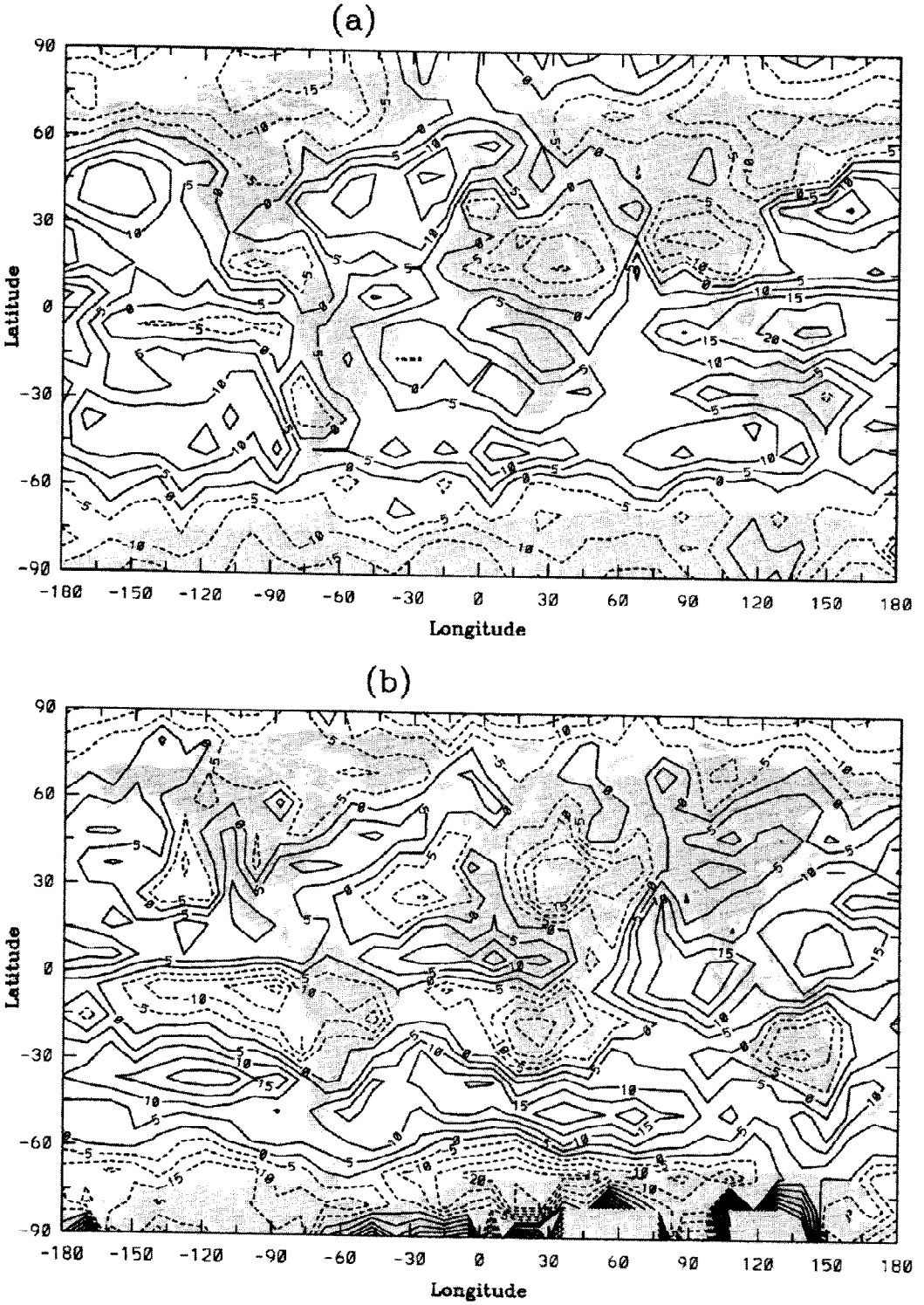

Figure 6. Global distribution of the deviation of the global mean fraction of two-layer cloudiness with an optically thin ($\tau < 1.0$) higher (Pc < 600 mbar) cloud layer over a lower (600 mbar < Pc < 900–950 mbar) cloud layer with around 100-mbar separation retrieved from HIRS analysis for (a) January 1990 and (b) July 1989. Global mean value is 24.3% for January 1990 and 31.0% for July 1989. Contour is plotted at 5.0% intervals, and the dashed lines indicate negative values.

marine stratiform cloud regions. Over land the fraction is larger in the summer than in the winter at all latitudes; over ocean it is larger in the summer for tropical and northern hemispheric eastern Pacific regions, while it is larger in the winter over other oceanic regions. Globally (excluding regions poleward of 60°), when a high cloud layer is present, the probability of a low cloud layer present below is 38% over land and 59% over ocean for January 1990 and is 53% over land and 76% over ocean for July 1989; this probability also varies geographically and seasonally.

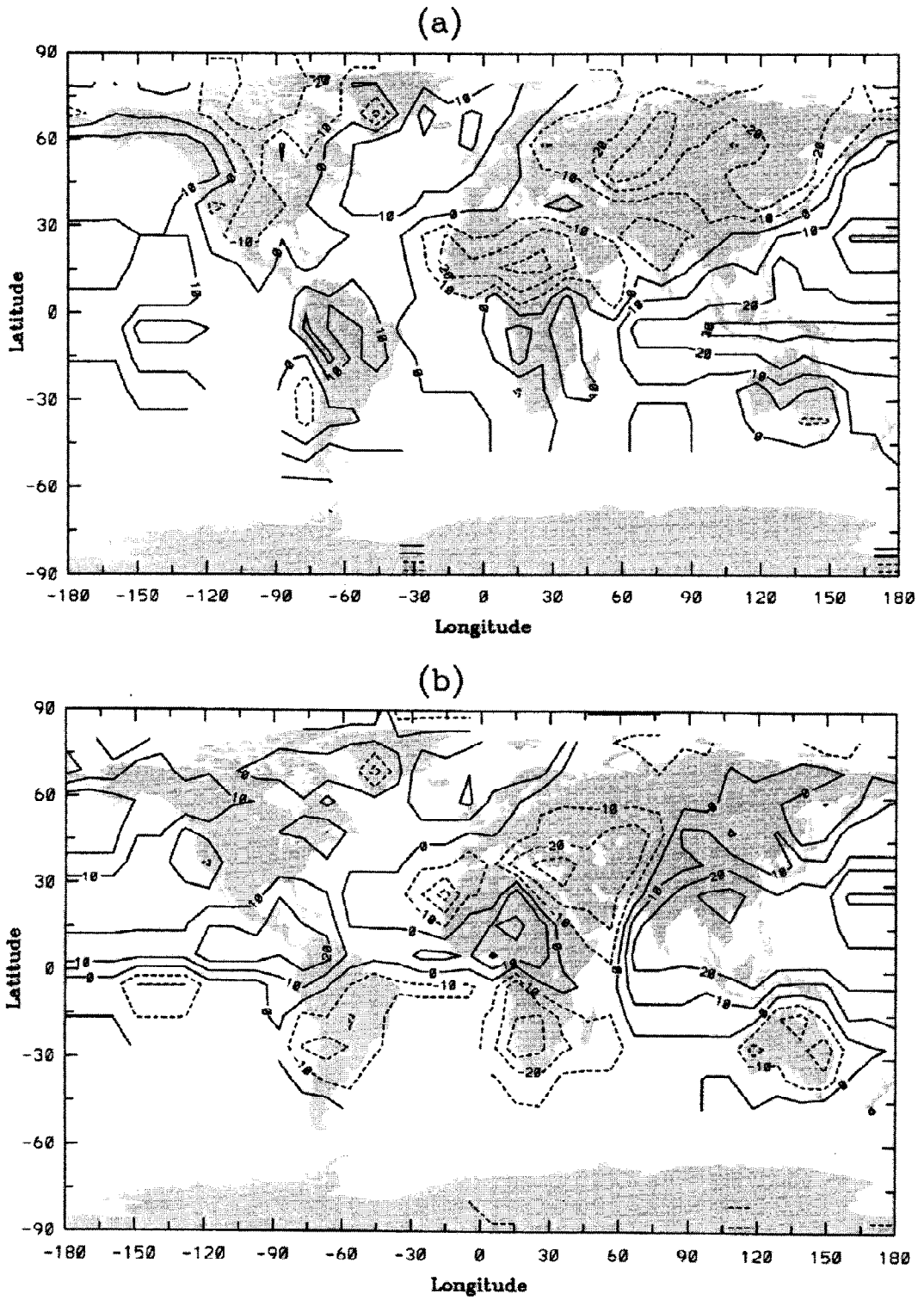

Figure 7. Global distribution of the deviation of the global mean fraction of multilayered clouds from the climatology of surface observation [*Hahn et al.*, 1982] for (a) winter seasonal average (December, January, and February) and (b) summer seasonal average (June, July, and August). Global mean value is 50.4% for the summer season and is 45.9% for the winter season. Contour is plotted at 10.0% intervals, and the dashed lines indicate negative values.

These results are sufficiently encouraging to do further studies of cloud vertical structure using satellite data, especially by combining several data sets. However, surface and upper air observations of cloud vertical structure are still needed to evaluate satellite retrieval results. Particularly important will be comparison with collections of cloud radar results when they become more extensive [cf. *Uttal et al.*, 1992; *Uttal and Frisch*, 1994].

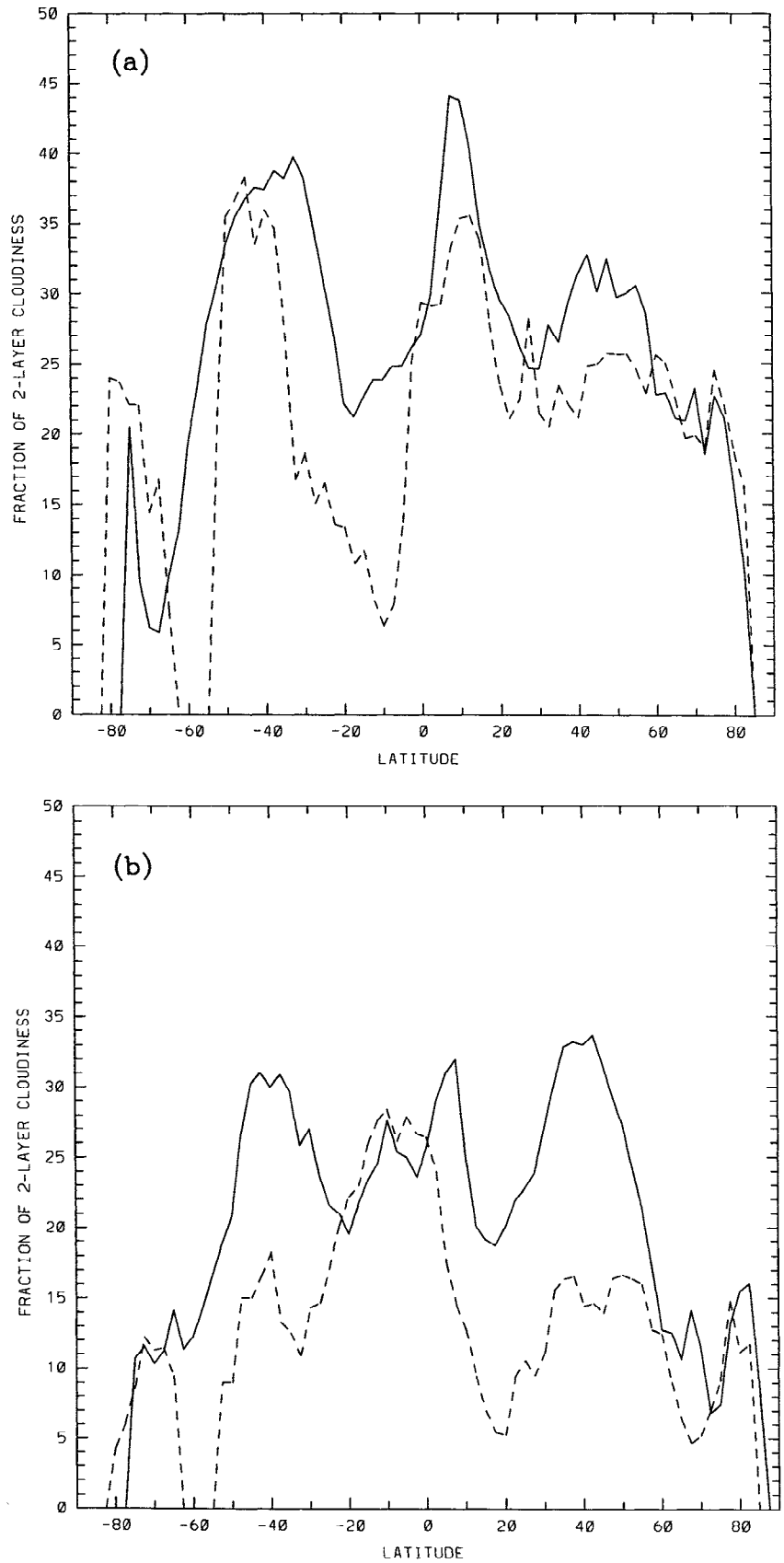

Figure 8. Latitudinal distribution of the fraction of two-layer cloudiness (solid line, over ocean; dashed line, over land) with an optically thin ($\tau < 1.0$) higher (Pc < 600 mbar) cloud layer over a lower (600 mbar) < Pc < 900–950 mbar) cloud layer with around 100-mbar separation retrieved from HIRS analysis for (a) July 1989 and (b) January 1990.

Acknowledgments. We want to thank Donald Wylie and Paul Menzel of University of Wisconsin-Madison for providing us with HIRS cloud analysis and Jeff Key of University of Colorado for instructions of using model Streamer. We also thank Donald Wylie, Claudia Stubenrauch, Qingyuan Han, and Junhong Wang for helpful discussions during the course of this study. This work was supported by the NASA Global Radiation Data Analysis and Modeling Program under Robert Curran and Robert Schiffer.

References

Baum, B. A., and B. A. Wielicki, Cirrus cloud retrieval using infrared sounding data: Multilevel cloud errors, *J. Appl. Meteorol.*, *33*, 107–117, 1994.

Baum, B. A., B. A. Wielicki, P. Minnis, and S. C. Tsay, Multilevel cloud retrieval using multispectral HIRS and AVHRR data: Nighttime oceanic analysis, *J. Geophys. Res.*, *99*, 5499–5514, 1994.

Buettner, K. J. K., and C. D. Kern, The determination of infrared emissivities of terrestrial surfaces, *J. Geophys. Res.*, *70*, 1329–1337, 1965.

Chahine, M. T., Remote sounding of cloudy atmospheres, I, The single cloud layer, *J. Atmos. Sci.*, *31*, 233–243, 1974.

Coakley, J. A., Jr., Properties of multilayered cloud systems from satellite imagery, *J. Geophys. Res.*, *88*, 10,818–10,828, 1983.

Coakley, J. A., Jr., and F. P. Bretherton, Cloud cover from high-resolution scanner data: Detecting and allowing for partially filled fields of view, *J. Geophys. Res.*, *87*, 4917–4932, 1982.

Cotton, W. R., and R. A. Anthes, *Storm and Cloud Dynamics*, *Int. Geophys. Ser.*, vol. 44, Academic, San Diego, Calif., 1989.

Ellingson, R. G., J. Ellis, and S. Fels, The intercomparison of radiation codes used in climate models: Long wave results, *J. Geophys. Res.*, *96*, 8929–8953, 1991.

Hahn, C. J., S. G. Warren, J. Gorgon, R. M. Chervin, and R. Jenne, Atlas of simultaneous occurrence of different cloud types over ocean, *NCAR Tech. Note TN-201+STR*, 212 pp., Natl. Cent. for Atmos. Res., Boulder, Colo., 1982.

Hahn, C. J., S. G. Warren, J. Gordon, R. M. Chervin, and R. Jenne, Atlas of simultaneous occurrence of different cloud types over land, *NCAR Tech. Note TN-241+STR*, 211 pp., Natl. Cent. for Atmos. Res., Boulder, Colo., 1984.

Jin, Y., W. B. Rossow, and D. P. Wylie, Comparison of the climatologies of high-level clouds from HIRS and ISCCP, *J. Clim.*, *9*, 2850–2879, 1996.

Key, J., Streamer user's guide, *Tech. Rep. 96-01*, 77 pp., Dep. of Geogr., Boston Univ., Boston, Mass., 1996.

Klein, S. A., and D. L. Hartmann, The seasonal cycle of low stratiform clouds, *J. Clim.*, *6*, 1587–1606, 1993.

Liao, X., W. B. Rossow, and D. Rind, Comparison between SAGE II and ISCCP high-level clouds, 1, Global and zonal mean cloud amounts, *J. Geophys. Res.*, *100*, 1121–1135, 1995a.

Liao, X., W. B. Rossow, and D. Rind, Comparison between SAGE II and ISCCP high-level clouds, 2, Locating cloud tops, *J. Geophys. Res.*, *100*, 1137–1147, 1995b.

Liu, G. S., J. A. Curry, and R. S. Sheu, Classification of clouds over the western equatorial Pacific Ocean using combined infrared and microwave satellite data, *J. Geophys. Res.*, *100*, 13,811–13,826, 1995.

McClatchey, R. A., R. W. Fenn, J. E. A. Selby, F. E. Voltz, and J. S. Garing, Optical properties of the atmosphere, *Rep. AFCRL-71-0279*, 85 pp., Air Force Cambridge Res. Lab., Bedford, Mass., 1971.

Menzel, W. P., W. L. Smith, and T. R. Stewart, Improved cloud motion wind vector and altitude using VAS, *J. Clim. Appl. Meteorol.*, *22*, 377–384, 1983.

Menzel, W. P., D. P. Wylie, and K. I. Strabala, Seasonal and diurnal changes in cirrus clouds as seen in four years of observations with the VAS, *J. Appl. Meteorol.*, *31*, 370–385, 1992.

Pinto, J. O., and J. Curry, Radiative characteristics of Arctic atmosphere during spring as inferred from ground-based measurements, *J. Geophys. Res.*, in press, 1996.

Poore, K., J. Wang, and W. B. Rossow, Cloud layer thickness from a combination of surface and upper-air observations, *J. Clim.*, *8*, 550–568, 1995.

Ramanathan, V., E. J. Pitcher, R. C. Malone, and M. L. Blackmon, The response of a spectral general circulation model to refinements in radiative processes, *J. Atmos. Sci.*, *40*, 605–630, 1983.

Randall, D. A., Harshvardhan, D. A. Dazlich, and T. G. Corsetti, Interactions among radiation, convection, and large-scale dynamics in a general circulation model, *J. Atmos. Sci.*, *46*, 1943–1970, 1989.

Rossow, W. B., and R. A. Schiffer, ISCCP cloud data products, *Bull. Am. Meteorol. Soc.*, *72*, 2–20, 1991.

Salisbury, J. W., and D. M. D'Aria, Emissivity of terrestrial materials in the 8–14 μm atmospheric window, *Remote Sens. Environ.*, *42*, 83–106, 1992.

Sheu, R.-S., J. Curry, and G. S. Liu, Vertical stratification of tropical cloud properties as determined from satellite, *J. Geophys. Res.*, in press, 1996.

Slingo, A., and J. M. Slingo, The response of a general circulation model to cloud longwave radiative forcing, I, Introduction and initial experiments, *Q. J. R. Meteorol. Soc.*, *114*, 1027–1062, 1988.

Smith, W. L., and C. M. R. Platt, Intercomparison of radiosonde, ground based laser, and satellite deduced cloud heights, *J. Appl. Meteorol.*, *17*, 1796–1802, 1978.

Tsay, S.-C., K. Stamnes, and K. Jayaweera, Radiative energy budget in the cloudy and hazy Arctic, *J. Atmos. Sci.*, *46*, 1002–1018, 1989.

Tian, L., and J. A. Curry, Cloud overlap statistics, *J. Geophys. Res.*, *94*, 9925–9935, 1989.

Uttal, T., and S. Frisch, Cloud boundaries during ASTEX, paper presented at Eighth Conference on Atmospheric Radiation, Am. Meteorol. Soc., Nashville, Tenn., 1994.

Uttal, T., E. E. Clothiaux, and T. P. Ackerman, Cloud boundary statistics during FIRE II, *J. Atmos. Sci.*, *52*, 4276–4284, 1992.

Wang, J. H., and W. B. Rossow, Determination of cloud vertical structure from upper-air observations, *J. Appl. Meteorol.*, *34*, 2243–2258, 1995.

Warren, S. G., C. J. Hahn, and J. London, Simultaneous occurrence of different cloud types, *J. Clim. Appl. Meteorol.*, *24*, 658–667, 1985.

Webster, P. J., and G. L. Stephens, Cloud-radiation interaction and the climate problem, in *The Global Climate*, edited by J. Houghton, pp. 63–78, Cambridge Univ. Press, New York, 1984.

Wylie, D. P., and W. P. Menzel, Two years of cloud cover statistics using VAS, *J. Clim.*, *2*, 380–392, 1989.

Wylie, D. P., and W. P. Menzel, A cirrus cloud climatology from NOAA/HIRS, *Palaeogeogr. Palaeoclimatol. Palaeoecol.*, *90*, 49–53, 1991.

Wylie, D. P., W. P. Menzel, H. M. Woolf, and K. I. Strabala, Four years of global cirrus cloud statistics using HIRS, *J. Clim.*, *7*, 1972–1986, 1994.

Yeh, H. Y., and K. N. Liou, Remote sounding of cloud parameters from a combination of infrared and microwave channels, *J. Clim. Appl. Meteorol.*, *22*, 201–213, 1983.

Y. Jin, Department of Geosciences, Columbia University, 2880 Broadway, New York, NY 10025. (e-mail: ciyxj@nasagiss.giss.nasa.gov)

W. B. Rossow, NASA Goddard Institute for Space Studies, 2880 Broadway, New York, NY 10025. (e-mail: clwbr@giss.nasa.gov)

(Received February 23, 1996; revised August 16, 1996; accepted September 23, 1996.)